Journal of Molecular Structure 935 (2009) 102–109

Contents lists available at ScienceDirect

Journal of Molecular Structure

journal homepage: www.elsevier.com/locate/molstruc

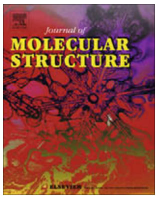

From diacetylferrocene to 1,1′-ferrocenyldiimines: Substituent effects on synthesis, molecular structure, electrochemical behavior and optical absorption property

Ting-Yu Lee [a,*], Pui-Ren Chiang [a,b], Ming-Chen Tsai [a,b], Che-Yu Lin [c], Jui-Hsien Huang [c]

[a] *Department of Applied Chemistry, National University of Kaohsiung, Kaohsiung 811, Taiwan*
[b] *Department of Chemistry, National Sun Yat-sen University, Kaohsiung 804, Taiwan*
[c] *Department of Chemistry, National Changhua University of Education, Changhua 500, Taiwan*

ARTICLE INFO

Article history:
Received 10 April 2009
Received in revised form 26 June 2009
Accepted 29 June 2009
Available online 4 July 2009

Keywords:
Ferrocenyldiimine
Acetylferrocenylimine
Condensation reaction
Electrochemical property
Hammett constant

ABSTRACT

A series of 1,1′-ferrocenyldiimines [$\mathrm{Fe\{(\eta^5\text{-}C_5H_4)\text{–}C(Me)N\text{–}R\}_2}$], where R = *n*-hexyl **1a**, cyclohexyl **1b**, phenyl **1c**, 4-methoxyphenyl **1d**, 3-methoxyphenyl **1e**, 4-nitrophenyl **1f**, and 3-nitrophenyl **1g**, have been synthesized by reactions of *ca.* 1:2 M ratio of 1,1′-diacetylferrocene and the corresponding amines. While *ca.* 1:1 M ratio of the starting materials was employed, acetylferrocenylimines [$\mathrm{Fe\{(\eta^5\text{-}C_5H_4)\text{–}C(CH_3){=}O\}\{(\eta^5\text{-}C_5H_4)\text{–}C(CH_3){=}N\text{–}R\}}$], where R = 4-nitrophenyl **2f**, and 3-nitrophenyl **2g**, were obtained. Single crystal X-ray structural analysis revealed that the two cyclopentadienyl rings in **1d**, **1e**, **1g**, **2f**, and **2g** were antiperiplanar staggered, anticlinal eclipsed, anticlinal eclipsed/synclinal eclipsed, synclinal eclipsed, and synclinal eclipsed to each other in solid state, respectively. All synthesized ferrocene derivatives exhibited a reversible one-electron redox process in their cyclic voltammograms, and the values of their redox potentials relied on the R groups. The correlation between the redox potential and the Hammett substituent constant, σ_p was quite well, with a correlation coefficient of 0.98. The UV–vis spectra showed that their optical property was also substituent dependent.

1. Introduction

Since the discovery of ferrocene [1], $(\eta^5\text{-}C_5H_5)_2Fe$, an increasing interest has been devoted to this prominent compound and its derivatives because of their wide application in catalysis, molecular electronics, polymer chemistry, nonlinear optical materials, and bioorganometallic materials [2–14]. Most of the derivatives were prepared by introducing functional groups into the cyclopentadienyl rings of ferrocene in order to tune their properties. One of intriguing research areas was therefore associated to 1,1′-disubstituted ferrocenes bearing nitrogen atoms as ligands primarily due to their distinctive geometry for application in organic synthesis and self-assembly materials [15–18]. Among these, the imino derivatives have demonstrated their fascinating coordination nature. For example, the reaction of 1,1′-ferrocenyldiimines with alkali-tetrachloropalladate salts produced cyclopalladated complexes containing $\sigma(\mathrm{Pd{-}C_{sp2,ferrocene}})$ bonds [19,20], which showed high catalytic activities for Heck reactions [21]. This metalation reaction followed by treatment with Lewis base, e.g., PPh_3, afforded two stereoisomers, *meso*- and D,L-bis(cyclopalladated) derivatives [19,20]. Mono-metalation might take place along with the hydrolysis of one imino group to form monocyclopalladate compound containing a carbonyl group on the other cyclopentadienyl ring [19,22]. Furthermore, expansion of the number of coordination sites on the imino groups of the derivatives might provide more diverse chelating modes as ligands with other metal ions. For instance, a ferrocenyl-containing pyridylimine-based bis-bidentate units and copper salt might undergo self-assembly process to yield a helical coordination polymer [23]. Moreover, dinuclear double-helical and mononuclear copper complexes with the ferrocenyl entity were prepared from the corresponding ferrocene derivatives with azine backbone chains [24]. The 1,1′-ferrocenyldiimines were also readily reduced to give amino-ferrocenyl analogues, which was potentially as precursors for molecular shuttle materials [25]. Although the method to prepare 1,1′-ferrocenyldiimines was reported, the individual reaction condition needed to be modified upon the substituents on imines [19]. Owing to the importance of these substances, the development of the strategy in preparation of 1,1′-ferrocenyldiimines has been still in progress [26]. Therefore, it is worthy to systematically study the synthetic process from the common starting material, diacetylferrocene to 1,1′-ferrocenyldiimines, especially from both the structural and electronic point of view. In addition, this scrutiny might benefit an opportunity to isolate possible intermediates, acetylferrocenylimines, which were potentially able to serve as N,O-heteroatom chelating ligands. On account of the potential application of

---

* Corresponding author. Tel.: +886 7 5919465; fax: +886 7 5919348.
E-mail address: tingyulee@nuk.edu.tw (T.-Y. Lee).

0022-2860/$ - see front matter © 2009 Elsevier B.V. All rights reserved.
doi:10.1016/j.molstruc.2009.06.047

1,1′-ferrocenyldiimines in biosensor and nonlinear optical material [27,28], it is also useful to investigate their electrochemical and optical properties. In this article, the synthesis, structures, electrochemical behavior, and optical absorption property of a series of 1,1′-ferrocenyldiimines and two novel acetylferrocenylimines are reported.

2. Experimental

2.1. Materials

Aniline (Aldrich), hexylamine (Aldrich), *m*-anisidine (Alfa Aesar), *p*-anisidine (Alfa Aesar), 3-nitroaniline (Alfa Aesar), 4-nitroaniline (Alfa Aesar), cyclohexylamine (Sigma–Aldrich), ferrocene (Alfa Aesar), toluene (Mallinckrodt Chemicals) and anhydrous magnesium sulfate (Shimakyu's pure chemicals) were used as received. Activated Al_2O_3 (Macherey–Nagel) was heated at 110 °C in an oven overnight before used. 1,1′-Diacetylferrocene was synthesized according to literature [29].

2.2. General procedure for synthesis of 1,1′-ferrocenyldiimines (**1a–g**) and acetylferrocenylimines (**2f** and **2g**)

Preparation of 1,1′-ferrocenyldiimines were modified by literature methods [19,30]. A Schlenk flask equipped with a Dean–Stark trap was charged with 1equiv of 1,1′-diacetylferrocene, 2.2 equiv of the selected amine, and toluene in the presence of freshly activated Al_2O_3 with or without $MgSO_4$. The mixture was refluxed from 24 to 72 h under nitrogen atmosphere. After filtration through Celite, the solvent and excess amines were removed to give compound **1**. The solid products were recrystallized from CH_2Cl_2/hexane. Under the similar reaction conditions, 1:1.1 M ratio of 1,1′-diacetylferrocene and the corresponding amines was employed to give compound **2** after recrystallization.

2.2.1. $[Fe\{(\eta^5\text{-}C_5H_4)\text{—}C(CH_3)\text{=}N\text{—}C_6H_{13}\}_2]$ (**1a**)

Without $MgSO_4$. 72 h. Red oil (yield = 95%). ^1H NMR (300 MHz, $CDCl_3$, rt): δ (ppm) 4.56 (4H, t, *J* = 1.8 Hz), 4.24 (4H, t, *J* = 2.1 Hz), 3.30 (4H, t, *J* = 7.5 Hz), 2.04 (6H, s, CH_3), 1.71–1.53 (4H, m), 1.44–1.15 (12H, m), 0.89 (6H, t, *J* = 6.6 Hz). $^{13}C\{^1H\}$ NMR (75 MHz, $CDCl_3$, rt): δ (ppm) 164.68 (CN), 87.04, 70.78, 68.44 (cyclopentadienyl), 51.98, 31.84, 30.86, 27.43, 22.72, 14.12 (*n*-hexyl), 15.84 (CH_3). Anal. calcd. for $C_{26}H_{40}FeN_2$: C, 71.55; H, 9.73; N, 6.42; found: C, 72.13; H, 9.73; N, 6.51%.

2.2.2. $[Fe\{(\eta^5\text{-}C_5H_4)\text{—}C(CH_3)\text{=}N\text{—}C_6H_{11}\}_2]$ (**1b**)

With $MgSO_4$. 72 h. Red oil (yield = 66%). ^1H NMR (300 MHz, $CDCl_3$, rt): δ (ppm) 4.52 (4H, t, *J* = 1.8 Hz), 4.22 (4H, t, *J* = 2.1 Hz), 3.41–3.29 (2H, m), 2.09 (6H, s, CH_3), 1.84–1.17 (20H, m). $^{13}C\{^1H\}$ NMR (75 MHz, $CDCl_3$, rt): δ (ppm) 162.21 (CN), 87.49, 70.69, 68.70 (cyclopentadienyl), 59.60, 33.69, 25.80, 24.99 (cyclohexyl), 15.79 (CH_3). Anal. calcd. for $C_{26}H_{36}FeN_2$: C, 72.22; H, 8.39; N, 6.48; found: C, 71.98; H, 8.12; N, 6.32%.

2.2.3. $[Fe\{(\eta^5\text{-}C_5H_4)\text{—}C(CH_3)\text{=}N\text{—}C_6H_5\}_2]$ (**1c**) [19]

With $MgSO_4$. 24 h. Orange solid (yield = 87%). ^1H NMR (300 MHz, $CDCl_3$, rt): δ (ppm) 7.28 (4H, t, *J* = 7.8 Hz), 7.03 (2H, t, *J* = 7.8 Hz), 6.73 (4H, dd, *J* = 8.4 Hz), 4.78 (4H, t, *J* = 2.1 Hz), 4.46 (4H, t, *J* = 2.1 Hz), 2.12 (6H, s, CH_3). $^{13}C\{^1H\}$ NMR (75 MHz, $CDCl_3$, rt): δ (ppm) 166.87 (CN), 151.57, 128.86, 123.06, 119.65 (aryl), 85.04, 71.86, 69.53 (cyclopentadienyl), 18.16 (CH_3). EI mass spectrum (*m*/*z*): 420 (M^+). Anal. calcd. for $C_{26}H_{24}FeN_2$: C, 74.30; H, 5.75; N, 6.66; found: C, 74.13; H, 6.02; N, 6.65. m.p. = 143–145 °C.

2.2.4. $[Fe\{(\eta^5\text{-}C_5H_4)\text{—}C(CH_3)\text{=}N\text{—}C_6H_4\text{-}4\text{-}OCH_3\}_2]$ (**1d**)

Without $MgSO_4$. 48 h. Red solid (yield = 61%). ^1H NMR (300 MHz, $CDCl_3$, rt): δ (ppm) 6.83 (4H, dd, *J* = 8.7 Hz), 6.68 (4H, dd, *J* = 8.7 Hz), 4.76 (4H, t, *J* = 1.8 Hz), 4.44 (4H, t, *J* = 1.8 Hz), 3.78 (6H, s, OMe), 2.13 (6H, s, CH_3). $^{13}C\{^1H\}$ NMR (75 MHz, $CDCl_3$, rt): δ (ppm) 167.10 (CN), 155.75, 144.75, 120.93, 114.13 (aryl), 85.32, 71.73, 69.42 (cyclopentadienyl), 55.46 (OMe), 18.09 (CH_3). EI mass spectrum (*m*/*z*): 480 (M^+). m.p. = 177–179 °C.

2.2.5. $[Fe\{(\eta^5\text{-}C_5H_4)\text{—}C(CH_3)\text{=}N\text{—}C_6H_4\text{-}3\text{-}OCH_3\}_2]$ (**1e**)

Without $MgSO_4$. 48 h. Red solid (yield = 62%). ^1H NMR (300 MHz, $CDCl_3$, rt): δ (ppm) 7.18 (2H, t, *J* = 8.1 Hz), 6.59 (2H, dd, *J* = 4.8 Hz), 6.33 (2H, d, *J* = 0.9 Hz), 6.30 (2H, d, *J* = 1.8 Hz), 4.77 (4H, t, *J* = 2.1 Hz), 4.45 (4H, *J* = 2.1 Hz), 3.73 (6H, s, OMe), 2.13 (6H, s, CH_3). $^{13}C\{^1H\}$ NMR (75 MHz, $CDCl_3$, rt): δ (ppm) 167.01 (CN), 160.21, 153.01, 129.67, 112.03, 108.72, 105.30 (aryl), 84.94, 71.88, 69.59 (cyclopentadienyl), 55.22 (OMe), 18.17 (CH_3). EI mass spectrum (*m*/*z*): 480 (M^+). Anal. calcd. for $C_{28}H_{28}N_2O_2Fe$: C, 70.01; H, 5.83; N, 5.87; found: C, 70.10; H, 5.82; N, 5.76. m.p. = 123–125 °C.

2.2.6. $[Fe\{(\eta^5\text{-}C_5H_4)\text{—}C(CH_3)\text{=}N\text{—}C_6H_4\text{-}4\text{-}NO_2\}_2]$ (**1f**)

With $MgSO_4$. 48 h. Yellow–orange solid (yield = 10%). ^1H NMR (300 MHz, $CDCl_3$, rt): δ (ppm) 8.16 (4H, dd, *J* = 8.7 Hz), 6.81 (4H, dd, *J* = 8.7 Hz), 4.78 (4H, t, *J* = 3 Hz), 4.53 (4H, t, *J* = 3 Hz), 2.11 (6H, s, CH_3). $^{13}C\{^1H\}$ NMR (75 MHz, $CDCl_3$, rt): δ (ppm) 167.89 (CN), 157.66, 143.66, 125.10, 119.75 (aryl), 83.84, 72.46, 70.03 (cyclopentadienyl), 18.57 (CH_3). EI mass spectrum (*m*/*z*): 510 (M^+). m.p. = 212–214 °C.

2.2.7. $[Fe\{(\eta^5\text{-}C_5H_4)\text{—}C(CH_3)\text{=}N\text{—}C_6H_4\text{-}3\text{-}NO_2\}_2]$ (**1g**)

Without $MgSO_4$. 48 h. Yellow–orange solid (yield = 50%). ^1HNMR (300 MHz, $CDCl_3$, rt): δ (ppm) 7.88 (2H, dd, *J* = 9.3 Hz), 7.57 (2H, t, *J* = 2.1 Hz), 7.41 (2H, t, *J* = 8.1 Hz), 7.04 (2H, dd, *J* = 8.1 Hz), 4.80 (4H, *J* = 1.8 Hz), 4.53 (4H, t, *J* = 1.8 Hz), 2.14 (6H, s, CH_3). $^{13}C\{^1H\}$ NMR (75 MHz, $CDCl_3$, rt): δ (ppm) 168.79 (CN), 152.49, 148.77, 129.68, 125.99, 117.97, 114.57 (aryl), 84.15, 72.307, 69.91 (cyclopentadienyl), 18.34 (CH_3). EI mass spectrum (*m*/*z*): 510 (M^+). Anal. calcd. for $C_{26}H_{22}N_4O_4Fe$: C, 61.19; H, 4.34; N, 10.98; found: C, 61.07; H, 4.81; N, 10.68. m.p. = 195–197 °C.

2.2.8. $[Fe\{(\eta^5\text{-}C_5H_4)\text{—}C(CH_3)\text{=}O\}\{(\eta^5\text{-}C_5H_4)\text{—}C(CH_3)\text{=}N\text{—}C_6H_4\text{-}4\text{-}NO_2\}]$ (**2f**)

Without $MgSO_4$. 48 h. Yellow–orange solid (yield = 50%). ^1HNMR (300 MHz, $CDCl_3$, rt): δ (ppm) 8.23 (2H, dd, *J* = 9 Hz), 6.92 (2H, dd, *J* = 9 Hz), 4.80 (4H, d, *J* = 1.8 Hz), 4.55 (2H, t, *J* = 2.1 Hz), 4.50 (2H, t, *J* = 0.9 Hz), 2.42 (3H, s), 2.06 (3H, s). $^{13}C\{^1H\}$ NMR (75 MHz, $CDCl_3$, rt): δ (ppm) 201.29 (CO), 167.55 (CN), 157.62, 143.59, 125.09, 120.14 (aryl), 84.12, 80.48, 73.36, 72.38, 70.99, 69.98 (cyclopentadienyl), 27.63 (CH_3—CO), 18.45 (CH_3). EI mass spectrum (*m*/*z*): 390 (M^+). m.p. = 169–171 °C.

2.2.9. $[Fe\{(\eta^5\text{-}C_5H_4)\text{—}C(CH_3)\text{=}O\}\{(\eta^5\text{-}C_5H_4)\text{—}C(CH_3)\text{=}N\text{—}C_6H_4\text{-}3\text{-}NO_2\}]$ (**2g**)

Without $MgSO_4$. 48 h. Yellow–orange solid (yield = 60%). ^1HNMR (300 MHz, $CDCl_3$, rt): δ (ppm) 7.94 (1H, d, *J* = 7.2 Hz), 7.67 (1H, s), 7.50 (1H, t, *J* = 7.5 Hz), 7.18 (H, d, *J* = 7.8 Hz), 4.82 (4H, s), 4.56 (2H, s), 4.49 (2H, s), 2.43 (3H, s), 2.07 (3H, s). $^{13}C\{^1H\}$ NMR (75 MHz, $CDCl_3$, rt): δ (ppm) 201.60 (CO), 168.49 (CN), 152.50, 148.83, 129.76, 126.33, 118.06, 114.82 (aryl), 84.44, 80.44, 73.37, 72.34, 70.94, 69.90 (cyclopentadienyl), 27.66 (CH_3–CO), 18.23 (CH_3). EI mass spectrum (*m*/*z*): 390 (M^+). m.p. = 150–152 °C.

2.3. Physical measurements

^1H and ^{13}C NMR spectra were obtained on a Varian Mercury 300 Plus spectrometer. Chemical shifts for ^1H and ^{13}C spectra were

Table 1
Summary of crystallographic data for compounds **1d**, **1e**, **1g**, **2f**, and **2g**.

	1d	**1e**	**1g**	**2f**	**2g**
Formula	$C_{28}H_{28}FeN_2O_2$	$C_{28}H_{28}FeN_2O_2$	$C_{52}H_{44}Fe_2N_8O_8$	$C_{20}H_{18}FeN_2O_3$	$C_{20}H_{18}FeN_2O_3$
M_w	480.37	480.37	1020.65	390.21	390.21
T (K)	150(2)	150(2)	150(2)	150(2)	150(2)
Crystal system	Monoclinic	Orthorhombic	Monoclinic	Monoclinic	Monoclinic
Space group	$P2(1)/n$	$P2(1)2(1)2(1)$	$C2/c$	$P2(1)/n$	$P2(1)$
a (Å)	6.9333(3)	8.5576(2)	15.1756(7)	10.6022(2)	9.209(2)
b (Å)	11.6867(5)	11.0220(3)	21.2914(10)	12.6707(3)	9.962(3)
c (Å)	14.1767(5)	24.0862(7)	14.5515(8)	13.5818(3)	9.314(2)
α (°)	90	90	90	90	90
β (°)	100.656(2)	90	100.008(3)	111.3050(10)	91.670(12)
γ (°)	90	90	90	90	90
V (Å^3)	1128.89(8)	2271.86(10)	4630.2(4)	1699.85(6)	854.2(4)
Z	2	4	4	4	2
d_c (Mg/m^3)	1.413	1.404	1.464	1.525	1.517
μ (mm$^{-1)}$	0.697	0.693	0.693	0.910	0.906
$F(0\,0\,0)$	504	1008	2112	808	404
Cryst. size	0.28 × 0.25 × 0.21	0.38 × 0.28 × 0.22	0.36 × 0.29 × 0.22	0.38 × 0.33 × 0.28	0.33 × 0.25 × 0.18
λ (Å)	0.71073	0.71073	0.71073	0.71073	0.71073
No. of rflns collected	12,066	24,956	26,412	16,442	9030
Index rflns	2718 (R_{int} = 0.0163)	5421 (R_{int} = 0.0405)	5990 (R_{int} = 0.0340)	3244 (R_{int} = 0.0196)	4141 (R_{int} = 0.0399)
Data/restraints/params	2718/0/153	5421/0/302	5990/0/319	3244/0/237	4141/1/237
Goodness-of-fit on F^2	1.057	1.031	1.067	1.051	1.053
R_1[a], wR_2[b] ($I > 2\sigma(I)$)	0.0267, 0.0780	0.0340, 0.0747	0.0411, 0.1000	0.0258, 0.0681	0.0496, 0.1293
R_1[a], wR_2[b] (all data)	0.0292, 0.0795	0.0467, 0.0782	0.0903, 0.1128	0.0293, 0.0701	0.0614, 0.1340
Largest diff peak, hole (e/Å^3)	0.402, −0.290	0.272, −0.240	0.418, −0.389	0.308, −0.256	0.956, −0.582

[a] $R_1 = \Sigma|F_0| - |F_c|/\Sigma|F_0|$.
[b] $wR_2 = [\Sigma[\omega(F_0^2 - F_c^2)^2]/\Sigma[\omega(F_0^2)^2]]^{1/2}$.

recorded in ppm relative to the residual protons and ^{13}C of $CDCl_3$ (δ 7.24, 77.7). Mass spectra were recorded on Thermo Electron Corporation PolarisQ. Elemental analyses were performed on Heraeus CHN-OS Rapid at the Instrument Center, NCHU. Melting points (m.p.) were measured on a Fargo MP-2D melting point apparatus. Cyclic voltammetry (CV) measurements were performed on a CHI 611A Electrochemical Analyzer with an Ag/AgCl reference electrode, a Pt working electrode, and a Pt counterelectrode, the scan rate at 50 mVs^{-1}, measured for 10^{-3} M solutions in 0.1 M tetrabutylammonium hexafluorophosphate as electrolyte in 1:1 of CH_2Cl_2/CH_3CN. UV–vis spectra were recorded on a Beckman Coulter DU730 spectrophotometer.

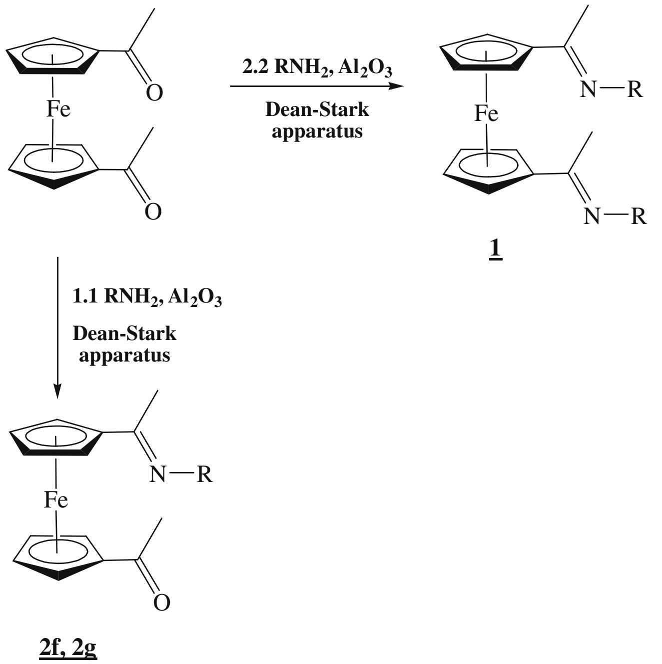

Scheme 1. R = *n*-hexyl (**a**), cyclohexyl (**b**), phenyl (**c**), 4-methoxyphenyl (**d**), 3-methoxyphenyl (**e**), 4-nitrophenyl (**f**), and 3-nitrophenyl (**g**).

2.4. Single crystal X-ray structure determination

Good diffraction quality single crystals of **1d**, **1e**, **1g**, **2f**, and **2g**, obtained by recrystallization from layering hexane over CH_2Cl_2 solutions, were mounted on a Bruker SMART CCD diffractometer equipped with graphite-monochromated Mo-K$_\alpha$ radiation (λ = 0.71073 Å), respectively. Crystal data were collected at 150 K with an Oxford Cryosystems Cryostream. No significant crystal decay was found. Data were corrected for absorption empirically by means of ψ scans. All non-hydrogen atoms were refined with anisotropic displacement parameters. For all the structures, the hydrogen atom positions were calculated and they were constrained to idealized geometries and treated as riding where the H atom displacement parameter was calculated from the equivalent isotropic displacement parameter of the bound atom. Data were processed using the CRYSALIS-CCD and -RED [31] programs. The structures of the complexes were determined by direct methods procedures in SHELXS [32a], and refined by full-matrix least-squares methods, on F^2's, in SHELXL [32b]. All the relevant crystallographic data and structure refinement parameters for **1d**, **1e**, **1g**, **2f**, and **2g** are summarized in Table 1.

3. Results and discussion

3.1. Reaction scheme and NMR spectra of compounds 1a–g, 2f, and 2g

A series of 1,1′-ferrocenyldiimines [Fe{(η^5-C_5H_4)—C(Me)=N—R}$_2$] with R = *n*-hexyl **1a**, cyclohexyl **1b**, phenyl **1c**, 4-methoxyphenyl **1d**, 3-methoxyphenyl **1e**, 4-nitrophenyl **1f**, and 3-nitrophenyl **1g**, were prepared by reactions of about 1:2 M ratio of 1,1′-diacetylferrocene and the corresponding amines, RNH_2, in the presence of freshly activated Al_2O_3 with or without $MgSO_4$ in refluxing toluene, equipped with a Dean–Stark apparatus (Scheme 1). This method was successful in the syntheses of the 1,1′-diimines, and no large excesses of the amines were necessary [19]. The increasing order of the difficulties of preparing theses ferrocenyldiimines was **1a** < **1c** < **1d** ≈ **1e** < **1b** < **1g** << **1f** according to the reaction time and yield. The electronic effect and the acid strength of the corresponding amines might play important roles in the condensation reaction, and therefore result in the very low yield (10%) of **1f**. The pK_a value of 4-nitroaniline is 1.00 [33]. The high yield of **1a** might be attributed to the steric, the electronic effect, and the high pK_a value of *n*-hexylamine (10.56) [33]. The protons on the η^5-C_5H_4 (Cp) rings of **1a–g** appear as two sets of signals in the range of δ 4.22–4.53 and δ 4.52–4.80 ppm respectively in their NMR spectra. Moreover, these signals were found to be downfield shifted as R = aryl with respect to those of R = *n*-hexyl and cyclohexyl. While substituents on the aryl moiety possess more electron-donating character, the proton resonance on η^5-C_5H_4 rings is upfield shifted. The ^{13}C NMR resonance of the imino carbon also shows downfield shifting as R = aryl, and further downfield shifting for compounds with electron-withdrawing groups on the aryl rings. The shifts of the NMR signals indicate that R groups possess noticeable electronic influence on both ferrocenyl and imino moieties.

Under the similar condition, the reaction of about 1:1 M ratio of 1,1′-diacetylferrocene with 4-nitroaniline and 3-nitroaniline resulted in **2f** and **2g**, respectively. The good yield (50%) of **2f** implied that the first acetyl group in diacetylferrocene would more readily experience the condensation reaction with 4-nitroaniline than the second one in the sequential reaction, which produced **1f** in low yield. On the other hand, the yields on preparing **1g** and **2g** were similar. The protons on the Cp rings of **2f** and **2g** show three signals in about 4.81, 4.55, and 4.50 ppm in their NMR spectra. The ^{13}C NMR resonance of the carbonyl (C=O) and the imino (C=N) group in **2f** and **2g** exhibits at *ca.* 201 and 168 ppm, respectively. Attempt to prepare other acetylferrocenylimines afforded a mixture of 1,1′-diacetylferrocene, the analogous 1,1′-ferrocenyldiimines, as well as the desired products, and further purification was not successful. The results are consistent with the facilitation of the condensation reaction as the R groups with more electron-rich character and higher pK_a value.

3.2. Crystal structures of compounds **1d**, **1e**, **1g**, **2f**, and **2g**

Crystals of **1d**, **1e**, **1g**, **2f**, and **2g** suitable for X-ray structure analysis were obtained by recrystallization from layering hexane over CH_2Cl_2 solutions of **1d**, **1e**, **1g**, **2f**, and **2g**. Their molecular structures are shown in Figs. 1–5. The selected bond lengths and angles are listed in Table 2. In view of the structures of the isomers of **1d** and **1e**, the Cp rings are approximately parallel with the tilt angles of 0° and 2.86°, respectively. Compound **1d** exhibits staggered Cp rings with an antiperiplanar arrangement of the two arylimino substituents. On the other hand, the two substituted Cp rings in **1e** are anticlinal eclipsed [34]. Similarly, the Cp rings of 1,1′-diacetylferrocene also exhibit anticlinal eclipsed arrangement [35]. The *N*-phenyl rings are almost perpendicular to their attached Cp rings for **1e**, the dihedral angles being 89.93° and 87.02°, however, those for **1d** are less upright with the dihedral angles of 79.58° and 79.58°. This arrangement renders little conjugation between the phenyl rings and the ferrocene motifs in the

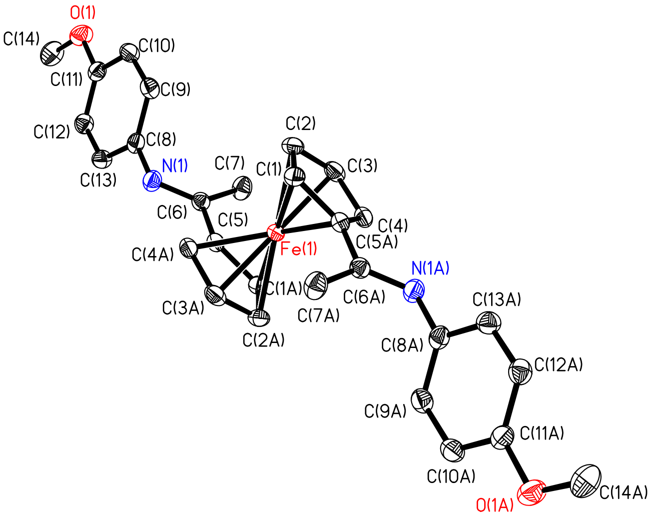

Fig. 1. Molecular structure of **1d**. The thermal ellipsoids are drawn at 50% probability levels and the hydrogen atoms were omitted for clarity.

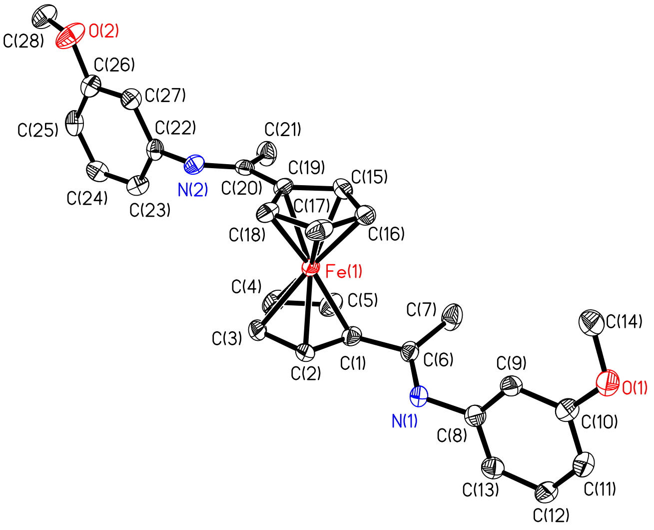

Fig. 2. Molecular structure of **1e**. The thermal ellipsoids are drawn at 50% probability levels and the hydrogen atoms were omitted for clarity.

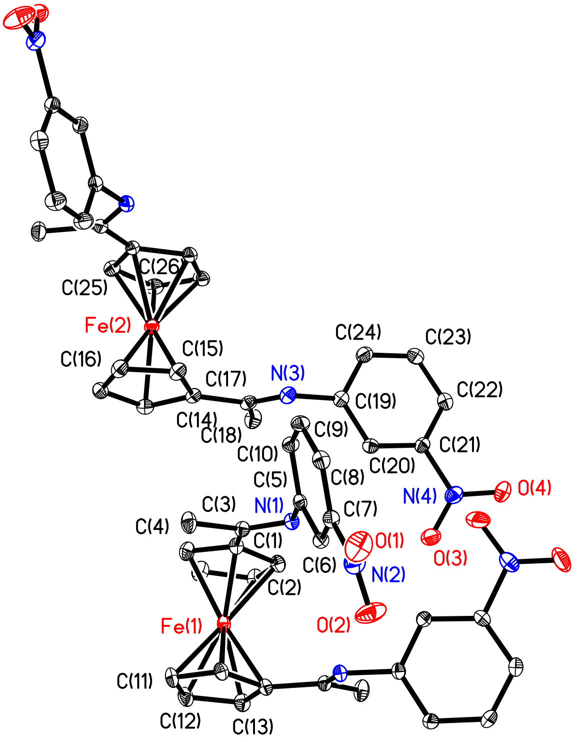

Fig. 3. Molecular structure of **1g**. The thermal ellipsoids are drawn at 30% probability levels and the hydrogen atoms were omitted for clarity.

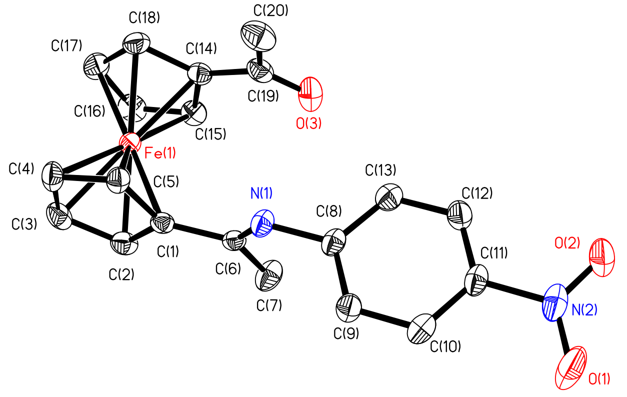

Fig. 4. Molecular structure of **2f**. The thermal ellipsoids are drawn at 50% probability levels and the hydrogen atoms were omitted for clarity.

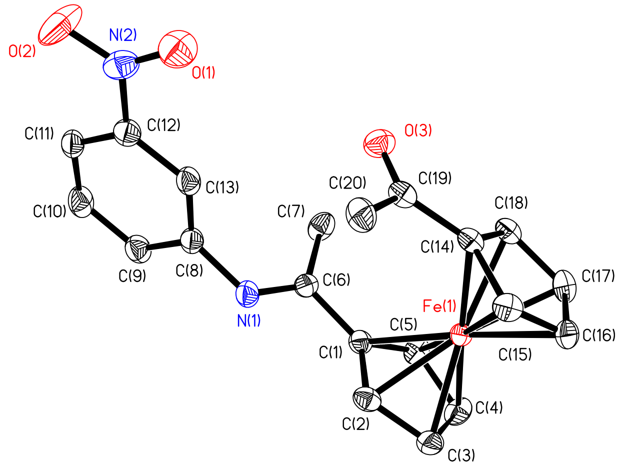

Fig. 5. Molecular structure of **2g**. The thermal ellipsoids are drawn at 50% probability levels and the hydrogen atoms were omitted for clarity.

Table 2
Selected bond lengths (Å) and angles (°) for compounds **1d**, **1e**, **1g**, **2f**, and **2g**.

1d			
C(5)—C(6)	1.467(2)	C(8)—C(13)	1.3922(17)
C(6)—N(1)	1.2853(15)	C(8)—N(1)	1.4158(18)
C(11)—O(1)	1.3708(16)	C(14)—O(1)	1.4262(17)
C(6)—C(7)	1.5144(17)		
N(1)—C(6)—C(5)	116.66(11)	N(1)—C(6)—C(7)	124.60(13)
C(5)—C(6)—C(7)	118.73(11)	C(6)—N(1)—C(8)	120.90(11)
C(11)—O(1)—C(14)	116.77(11)		
1e			
C(1)—C(6)	1.478(3)	C(6)—N(1)	1.279(3)
C(6)—C(7)	1.492(3)	C(8)—N(1)	1.422(3)
C(10)—O(1)	1.360(3)	C(14)—O(1)	1.429(3)
C(19)—C(20)	1.475(3)	C(20)—N(2)	1.282(3)
C(20)—C(21)	1.502(3)	C(22)—N(2)	1.415(3)
C(26)—O(2)	1.357(3)	C(28)—O(2)	1.431(3)
N(1)—C(6)—C(1)	116.19(19)	N(1)—C(6)—C(7)	125.79(19)
C(6)—N(1)—C(8)	121.71(18)	C(6)—N(1)—C(8)	121.71(18)
N(2)—C(20)—C(19)	116.10(19)	N(2)—C(20)—C(21)	125.7(2)
C(20)—N(2)—C(22)	121.92(19)	C(26)—O(2)—C(28)	117.07(18)
1g			
C(1)—C(3)	1.475(3)	C(3)—N(1)	1.277(2)
C(3)—C(4)	1.506(3)	C(3)—C(4)	1.506(3)
C(5)—N(1)	1.417(2)	C(14)—C(17)	1.477(3)
C(17)—N(3)	1.270(2)	C(19)—N(3)	1.425(2)
N(1)—C(3)—C(1)	117.93(17)	N(1)—C(3)—C(4)	125.51(18)
C(1)—C(3)—C(4)	116.56(18)	C(3)—N(1)—C(5)	119.08(16)
N(3)—C(17)—C(14)	118.35(18)	N(3)—C(17)—C(18)	125.22(19)
C(14)—C(17)—C(18)	116.42(18)	C(17)—N(3)—C(19)	119.79(17)
2f			
C(1)—C(6)	1.470(2)	C(6)—N(1)	1.279(2)
C(8)—N(1)	1.407(19)	C(19)—O(3)	1.220(2)
C(14)—C(19)	1.475(2)		
C(1)—C(6)—N(1)	117.48(13)	C(8)—N(1)—C(6)	121.50(13)
O(1)—N(2)—O(2)	123.28(15)	C(11)—N(2)—O(1)	118.40(16)
C(14)—C(19)—O(3)	120.03(16)		
2g			
C(1)—C(6)	1.473(5)	C(6)—N(1)	1.280(5)
C(8)—N(1)	1.417(4)	C(19)—O(3)	1.226(5)
C(14)—C(19)	1.470(5)		
C(1)—C(6)—N(1)	116.8(4)	C(8)—N(1)—C(6)	120.9(3)
O(1)—N(2)—O(2)	123.5(4)	C(12)—N(2)—O(1)	118.6(3)
C(14)—C(19)—O(3)	120.3(4)		

solid state. Such conformation was also found in the structures of the monoimino analogy, phenyliminoferrocene (**Fc-Ph**) and [1-[(4-chlorophenyl)imino]ethyl]ferrocene (**Fc-4-ClPh**) [30,36]. In comparison with the structures of 1,1′-bis(*N*-aryl-formimidoyl) ferrocenes (aryl = phenyl **Fc-Ph$_2$**, and 2,6-diisopropylphenyl **Fc-(^{i}pr-Ph)$_2$**), both *N*-aryl rings in **Fc-(^{i}pr-Ph)$_2$** show the similar perpendicularity; only one *N*-aryl rings in **Fc-Ph$_2$** is perpendicular to its Cp rings, but the other possesses a parallel conformation, which may result from a C—H…arene–π-interaction [37]. Moreover, the configuration of the two Cp rings in **Fc-(^{i}pr-Ph)$_2$** is anticlinal staggered, and that in **Fc-Ph$_2$** is synperiplanar eclipsed. The C=N bond length of the imino groups in **1d** and **1e** is *ca.* 1.28 Å, slightly longer than that in **Fc-Ph** (1.269(5) Å), and **Fc-4-ClPh** (1.263(6) Å), and **Fc-(^{i}pr-Ph)$_2$** (1.273(2) Å), which can be attributed to the difference of the substituents on the phenyl moiety. The imino functional groups in **1d** are oriented almost coplanar with their attached Cp rings with a dihedral angle C(4A)—C(5)—C(6)—N(1) *ca.* 22.53° (Fig. 1). The similar configuration was observed in **1e**, of which the dihedral angles C(2)—C(1)—C(6)—N(1) and C(18)—C(19)—(20)—N(1) are *ca.* 22.37° and *ca.* 10.89°, respectively (Fig. 2).

In the case of 3-nitro derivative, **1g**, two independent molecules are present in the unit cell (Fig. 3). The Cp rings in both species are planar and nearly parallel as the tilt angles in the range between 2.71° and 4.79°. Moreover, the first species with Fe(1) encloses synclinal eclipsed iminic Cp rings, and the second species contains anticlinal eclipsed substituted Cp rings. The results imply that the relationship of the two Cp rings is fluxional and the energy barrier for the interconversion of the different conformations between Cp rings is low. It has also been reported that the energy difference between the D_{5h} and D_{5d} conformations of ferrocene were 0.9 ± 0.3 kcal/mol [38]. A theoretical calculation also demonstrated that the energy difference between the eclipsed and staggered configurations of the monosubstituted ferrocenes is in a range between −0.54 and 0.41 kcal/mol [39]. The angles between the *N*-phenyl rings and their attached Cp rings for the two species in **1g** are quite distinct, being 66.67° and 84.50°, respectively. The conformation of Fe(1) species in **1g** suggests that little conjugation phenomenon between the phenyl rings and the ferrocene motifs might occur. The Cp rings and the imino moieties are roughly coplanar, as the dihedral angle C(2)—C(1)—C(3)—N(1) *ca.* 11.68° and C(15)—C(14)—C(17)—N(3) *ca.* 10.95°.

The X-ray structure of **2f** revealed that the two Cp rings are parallel (the tilt angle *ca.* 1.61°) and synclinal staggered (the twist angle *ca.* 30.5°) to each other (Fig. 4). The *N*-phenyl ring is nearly perpendicular to its attached Cp ring at the angle *ca.* 84.33°. The carbonyl group are almost coplanar with its attached Cp ring (the dihedral angle C(15)—C(14)—C(19)—O(3) *ca.* 13.54°) and so is the imino group (the dihedral angle C(5)—C(1)—C(6)—N(1) *ca.* 7.81°). The similar geometry was observed in **2g**, of which the tilt angle of the Cp rings is *ca.* 3.24°, the twist angle (synclinal staggered) is *ca.* 23–24°, and the angle between the *N*-phenyl ring and its attached Cp ring is *ca.* 74.67° (Fig. 5). The dihedral angles C(18)—C(14)—C(19)—O(3) being *ca.*

−2.31° and C(2)—C(1)—C(6)—N(1) being *ca.* −18.34° illustrated the coplanar relation between the carbonyl group and the imino group and their attached Cp rings, respectively.

With focus on the relative orientations of the bis(substituted) motifs in **1d**, **1e**, **1g**, **2f,** and **2g**, the conformational features are various by projecting down the Cp(centroid)—Fe—Cp(centroid) axis, sketched in Fig. 6 [40]. For the 1,1′-ferrocenyldiimines, the imino groups are closer to each other in **1g**, further in **1e**, and *anti* to each other in **1d**. The 3-methoxy and 3-nitro analogues favor an eclipsed configuration, but the 4-methoxy derivative retains a staggered form. The antiperiplanar and anticlinal conformations of the two imino moieties are observed in **1d**, **1e**, and **1f**. Therefore, the geometry of **1e** and **1f** is similar to that of 1,1′-diacetylferrocene [35]. However, the carbonyl and imino groups in **2f** and **2g** exhibit only the synclinal conformation, which might imply some interaction between the two groups. Although the Cp rings in **2f** and **2g** are staggered, the twist angles (23–30°) in both compounds are relatively smaller than the typical one, such as *ca.* 36° in **1d**. The C—C bond lengths within the η^5-Cp rings of the compound **1d**, **1e**, **1f**, **2f**, and **2g** are in a classic range between 1.400(4) Å and 1.442(3) Å as well as the Fe—C(Cp) bond distances of the five compounds are in a typical range between 2.027(2) Å and 2.063(5) Å. The results indicate that all the compound **1d**, **1e**, **1f**, **2f**, and **2g** possess the typical ferrocene structure [41].

*3.3. Electrochemical and optical properties of compounds **1a–g**, **2f**, and **2g***

All compounds **1** and **2** exhibit a typical reversible one-electron redox process attributed to a ferrocene/ferrocenium couple in their

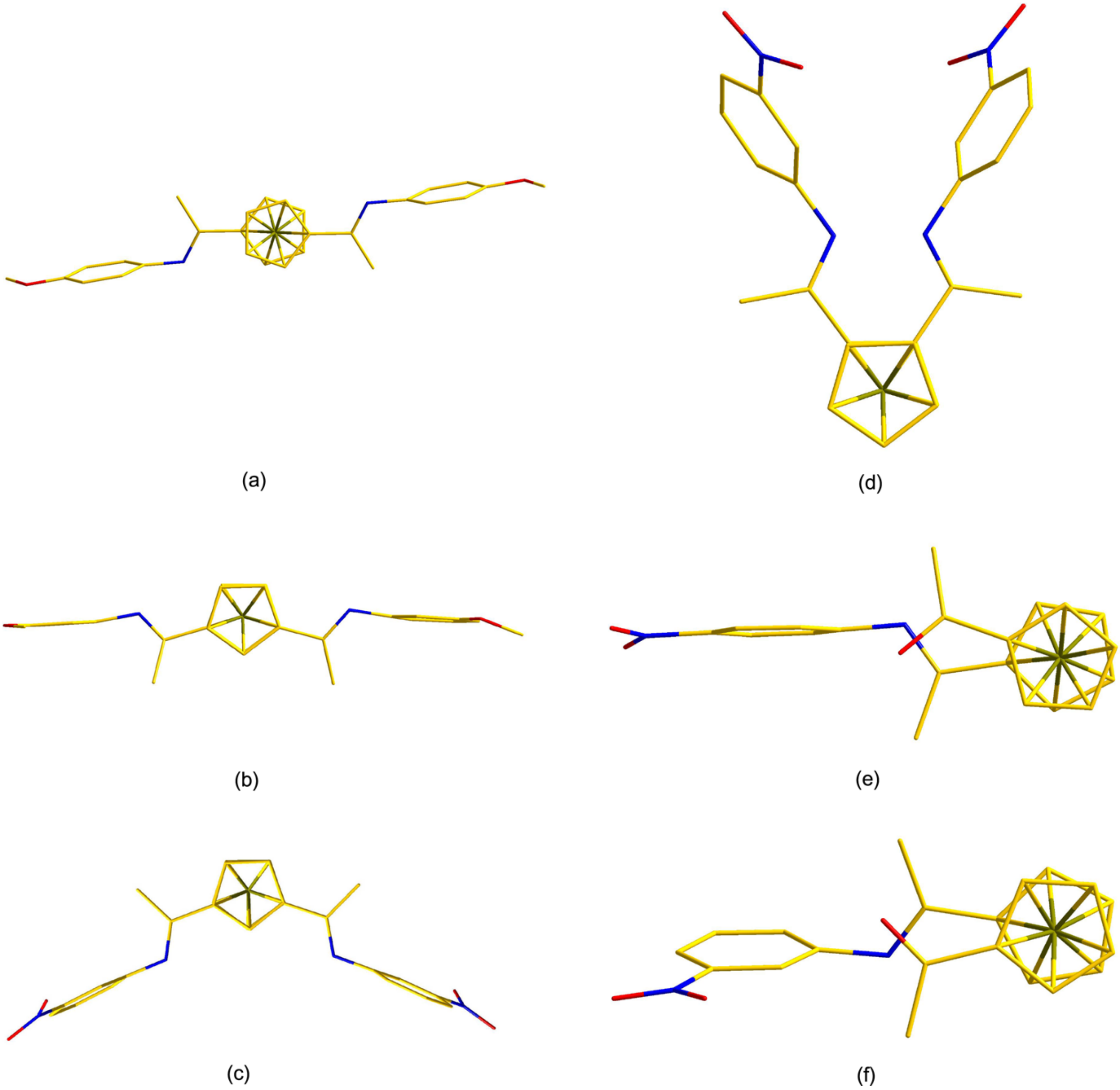
(a) (d) (b) (e) (c) (f)

Fig. 6. Conformation of the cyclopentadienyl rings of the ferrocene motifs in each of (a) **1d**, (b) **1e**, (c, d) **1g**, (e) **2f**, and (f) **2g**. The diagrams illustrate the relative dispositions of the five-membered rings as well as the orientations of the imino moieties in the five compounds.

Table 3
Measured $E_{1/2}$ values and the Hammett constants (σ_p) for compounds **1a–g**, **2f**, and **2g**.

Compound	$E_{1/2}$ (V)	Substituent (R)	σ_p[a]
1a	0.640	$(CH_2)_5CH_3$	–[b]
1b	0.597	Cyclo-C_6H_{11}	−0.15
1c	0.718	C_6H_5	−0.01
1d	0.674	C_6H_4—4-OMe	−0.08
1e	0.690	C_6H_4—3-OMe	–[b]
1f	0.864	C_6H_4—4-NO_2	0.26
1g	0.819	C_6H_4—3-NO_2	0.23
2f	0.831		
2g	0.818		
Ferrocene	0.429		
Diacetylferrocene	0.897		

[a] Ref. [45].
[b] Not found.

Table 4
The electronic transition bands in the UV/vis spectra of compounds **1a–g**, **2f**, **2g**, and **$1a^{ox}$–$1g^{ox}$** in CH_2Cl_2.

Compound	λ_{max}/nm (ε_{max}/mol^{-1} dm^3 cm^{-1})			
1a	232 (48,950)	268 (21,100)	328 (4100)	444 (1100)
1b	232 (40,500)	268 (19,150)	338 (3050)	459 (700)
1c	232 (30,500)	270 (14,600)	330 (5800)	446 (850)
1d	235 (41,500)	269 (20,900)	328 (11,200)	452 (1200)
1e	232 (27,050)	274 (12,000)	322 (5150)	450 (650)
1f	232 (57,700)	280 (24,300)	330 (45,400)	448 (2750)
1g	235 (23,600)	273 (12,940)	333 (4000)	446 (400)
$1a^{ox}$	235 (13,150)	294 (48,800)	364 (28,350)	505 (2000)
$1b^{ox}$	234 (13,150)	290 (48,000)	364 (28,050)	508 (1900)
$1c^{ox}$	238 (9700)	294 (25,350)	361(19,300)	503 (2150)
$1d^{ox}$	234 (16,400)	293 (35,600)	363 (25,500)	503 (3050)
$1e^{ox}$	234 (16,150)	293 (29,650)	362 (20,450)	500 (2550)
$1f^{ox}$	233 (22,200)	299 (19,450)	349 (27,200)	496 (2100)
$1g^{ox}$	236 (29,650)	286 (22,250)	358 (13,250)	499 (2000)

cyclic voltammograms [42]. The data of their redox potentials are listed in Table 3. The results show the order of their redox potentials as the following: ferrocene < **1b** < **1a** < **1d** < **1e** < **1c** < **2g** < **1g** < **2f** < **1f** < diacetylferrocene (Table 3). Generally, the aryl derivatives of the ferrocenyldiimines possess higher $E_{1/2}$ values than the alkyl derivatives. For the aryl-substituted ferrocenyldiimines, the species with the electron-withdrawing group (NO_2) on the phenyl rings have much larger redox potentials than those with the electron-donating group (OMe), indicating the electron-rich group facilitates the oxidation of the systems. The redox potential of compounds **1** is higher than that of ferrocene, but lower than that of diacetylferrocene, which illustrate that the electron-attracting ability of the imino group is stronger than hydrogen (H), but weaker than acetyl (C(O)Me) group. The correlation of the ferrocene/ferrocenium redox potential with Hammett constants has been used as a probe in study of the electronic properties of the substituents in ferrocenyl units [43]. Our results show that the redox potentials of the ferrocenyldiimines linearly correlate with the Hammett σ_p constants of the substituents R (Table 3 and Fig. 7) [44]: $E_{1/2} = 0.575\,\sigma_p + 0.706$, $r = 0.984$. Although the σ_p value of *n*-hexyl group is not available, the pK_a value (10.66) of cyclohexylamine higher than that of *n*-hexylamine (10.56) [33] is consistent with the lower $E_{1/2}$ value of **1b**. The correlation indicates that the influence of the R groups onto the ferrocene centers is efficient. The $E_{1/2}$ value of **1f** is higher than that of **2f** and **2g**, which suggests that the electronic effect of the 4-nitro group plays a significant role during the oxidation process and leads to the predicament of oxidation.

Optical spectroscopy is a power tool for studying the electronic structure of ferrocene. Basically, two kinds of electronic transition bands are observed: the Laporte-forbidden d–d character of ligand field transitions appearing at 325 nm (arising from the unresolved $^1A_{1g} \rightarrow a^1E_{1g}$ and $^1A_{1g} \rightarrow {}^1E_{2g}$ transitions) along with 440 nm (arising from the $^1A_{1g} \rightarrow b^1E_{1g}$ transition), and the intramolecular charge transfer transitions showing at 200, 240, along with 265 nm [45–47]. The d–d transition bands were found to be substituent dependent [48,49]. The data of the UV/vis absorption spectra of compounds 1a–g, **2f**, and **2g** are listed in Table 4. The bands (*ca.* 450 nm) are red-shifted in the order of **1a** < **1c** ≈ **1g** < **2g** < **1f** < **1e** < **1d** < **2f** < **1b**; however, the difference of the shifts are small. Only little change is observed at the bands (*ca.* 330 nm) as well. The results might reflect the substitution effect on the HOMO and LUMO energy levels as well as the consequential HOMO–LUMO gaps of ferrocenyldiimines and acetylferrocenylimines [39,50]. It is worthy to measure the electronic spectra of the ferrocenium ions due to their importance to the studies of electronic structure [51], biosensors [52], and antitumor activity [53]. The ferrocene derivatives could be oxidized by I_2 to form triiodide salts [51]. Our premier study showed that the optical absorption bands of the ferrocenium species **$1a^{ox}$**, which resulted from the reaction of **1a** and appropriate amount of I_2 were red-shifted compared to those of **1a** (Table 4 and Fig. 8). Similar phenomena were observed in **$2b^{ox}$–$2g^{ox}$**, the corresponding ferrocenium derivatives of **2b–2g**, and their data of the UV/vis absorption spectra were listed in Table 4. The position and the intensity of the bands at *ca.* 500 and 360 nm in **$2b^{ox}$–$2g^{ox}$** are almost the same, and therefore are assigned as essentially metal d–d transition [45,51]. No absorption bands were observed at lower-energy area (>600 nm) even at high concentration of the compounds. According to the UV–vis spectroscopy, the electronic structures of the ferrocenyldiimines are more complicated than those of the typical ferrocene derivatives.

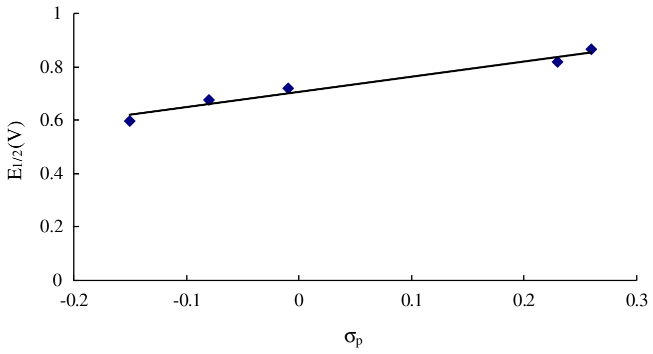

Fig. 7. Correlation between $E_{1/2}$ and the Hammett constants (σ_p's).

4. Conclusion

We demonstrated that Schiff-base condensation reaction of 1:2 M ratio of 1,1′-diacetylferrocene and the analogous amines in

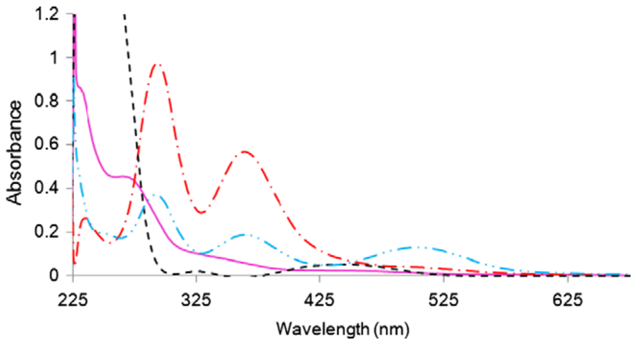

Fig. 8. UV–vis spectra of **1a** (pink, —), **$1a^{ox}$** (red, –·–), ferrocene (black, –), and ferrocenium (blue, –··–) for 2.5 x 10^{-4} M solutions in CH_2Cl_2. (For interpretation of the references to color in this figure legend, the reader is referred to the web version of this paper.)

the presence of freshly activated Al_2O_3 with or without $MgSO_4$ efficiently afford the ferrocenyldiimines, compound **1**. The yield was dependent on the electronic, acidic and steric property of the substituent of the amine. The group (4-nitrophenyl) with the most electron-withdrawing ability and the smallest pK_a value leaded to the lowest yield (10%). The less steric and acidic along with more electron-donating substituent such as *n*-hexyl group resulted in higher yield (95%). The pure acetylferrocenylimines **2f** and **2g** can be obtained by the reaction of 1:1 M ratio of 1,1′-diacetylferrocene and the amines with more electron-withdrawing feature such as 3-nitroaniline and 4-nitroaniline. The condensed molecular structures show that the Cp rings are parallel to the imino motifs and perpendicular to the *N*-phenyl rings. The two cyclopentadienyl rings in **1d**, **1e**, **1g**, **2f**, and **2g** exhibit an antiperiplanar staggered, anticlinal eclipsed, anticlinal eclipsed/synclinal eclipsed, synclinal eclipsed, and synclinal eclipsed conformation, respectively. The substituents on the imino parts strongly affect the redox potentials of the iron centers in the ferrocenyl segments according to the CV measurement. The stronger basicity of their corresponding amines, the lower redox potentials of the ferrocenyldiimines. Moreover, the correlation between the redox potential and the Hammett substituent constant, σ_p is quite well, with a correlation coefficient of 0.98. The UV–vis spectra also illustrate that the substituents affect their optical property.

5. Supplementary material

Crystallographic data for structural analysis has been deposited to the Cambridge Crystallographic Data Center, bearing CCDC 653774 (**1d**), CCDC 653775 (**2g**), CCDC 653776 (**2f**), CCDC 653777 (**1e**), and CCDC 653778 (**1g**). Copies of this information may be obtained free of charge from the Director, CCDC, 12 Union Road, Cambridge, CB2 IEZ, UK (fax: +44 1223 336 033; e-mail deposit@ccdc.cam.ac.uk or http://www.ccdc.cam.ac.uk).

Acknowledgements

We thank the National Science Council of Taiwan for financial support and the National Center for High Performance Computing for databank search. J.H.H. also thank the National Changhua University of Education for the purchase of the CAD-4 diffractometer system.

References

[1] (a) T.J. Kealy, P.L. Pauson, Nature 168 (1951) 1039;
(b) S.A. Miller, J.A. Tebboth, J.F. Tremaine, J. Chem. Soc. (1952) 632;
(c) G. Wilkinson, M. Rosenblum, M.C. Whiting, R.B. Woodward, J. Am. Chem. Soc. 74 (1952) 2125;
(d) E.O. Fischer, W.Z. Pfab, Naturforsch. B 7 (1952) 377.
[2] A. Togni, T. Hayashi (Eds.), Ferrocenes: Homogeneous Catalysis, Organic Synthesis, Material Science, VCH, New York, 1995.
[3] M. Horie, T. Sakano, K. Osakada, J. Organomet. Chem. 691 (2006) 5935.
[4] C. Lambert, V. Kriegisch, A. Terfort, B. Zeysing, J. Electroanal. Chem. 590 (2006) 32.
[5] S. Barlow, D. O'Hare, Chem. Rev. 97 (1997) 637.
[6] H.B. Kraatz, J. Inorg. Organomet. Polym. Mater. 15 (2005) 83.
[7] P. Nguyen, P. Go'mez-Elipe, L. Manners, Chem. Rev. 99 (1999) 1515.
[8] I. Manners, Science 294 (2001) 1664.
[9] C.T. Sanderson, B.J. Palmer, A. Morgan, M. Murphy, R.A. Dluhy, T. Mize, I.J. Amster, C. Kutal, Macromolecules 35 (2002) 9648.
[10] N.J. Long, Angew. Chem. Int. Ed. Engl. 34 (1995) 21.
[11] I. Manners, J. Opt. A: Pure Appl. Opt. 4 (2002) S221.
[12] C. Paquet, P.W. Cyr, E. Kumacheva, I. Manners, Chem. Commun. (2004) 234.
[13] C. Padeste, B. Steiger, A. Grubelnik, L. Tiefenauer, Biosen. Bioelectron. 20 (2004) 545.
[14] D.R. Van Staveren, N. Metzler-Nolte, Chem. Rev. 104 (2004) 5931.
[15] L.X. Dai, T. Tu, S.L. You, W.P. Deng, X.L. Hou, Acc. Chem. Res. 36 (2003) 659.
[16] O.B. Sutcliffe, M.R. Bryce, Tetrahedron: Asymmetry 14 (2003) 2297.
[17] H. Sato, J. Anzai, Biomacromolecules 7 (2006) 2072.
[18] J.-L. Syssa-Magalé, K. Boubekeurb, P. Palvadeaub, A. Meerschautb, B. Schöllhorn, J. Mol. Struct. 691 (2004) 79.
[19] R. Bosque, C. López, J. Sales, X. Solans, M. Font-Bardia, Organometallics 18 (1999) 1267.
[20] Y.J. Wu, Y.H. Liu, L. Yang, Q. Zhu, Polyhedron 16 (1997) 335.
[21] Y.J. Wu, J.J. Hou, H.Y. Yun, X.L. Cui, R.J. Yuan, J. Organomet. Chem. 637–639 (2001) 793.
[22] C. Xu, J.F. Gong, Y.H. Zhang, Y. Zhu, C.X. Du, Y.J. Wu, Inorg. Chem. Commun. 9 (2006) 456.
[23] C.J. Fang, C.Y. Duan, D. Guo, C. He, Q.J. Meng, Z.M. Wang, C.H. Yan, Chem. Commun. (2001) 2540.
[24] C.J. Fang, C.Y. Duan, H. Mo, C. He, Q.J. Meng, Y.J. Liu, Y.H. Mei, Z.M. Wang, Organometallics 20 (2001) 2525.
[25] M. Horie, Y. Suzaki, K. Osakada, Inorg. Chem. 44 (2005) 5844.
[26] C. Imrie, P. Kleyi, V.O. Nyamori, T.I.A. Gerber, D.C. Levendis, J. Look, J. Organomet. Chem. 692 (2007) 3443.
[27] (a) M. Zamora, S. Herrero, J. Losada, I. Cuadrado, C.M. Casado, B. Alonso, Organometallics 26 (2007) 2688;
(b) H.C. Yoon, M.Y. Hong, H.S. Kim, Anal. Chem. 72 (2000) 4420.
[28] I. Ratera, D. Ruiz-Molina, C. Sánchez, R. Alcalá, C. Rovira, J. Veciana, Synthetic Met. 121 (2001) 1834.
[29] M.A. Carroll, A.J.P. White, D.A. Widdowson, D.J. Williams, J. Chem. Soc. Perkin Trans. 1 (2000) 1551.
[30] R. Bosque, C. López, J. Sales, X. Solans, M. Font-Bardía, J. Chem. Soc. Dalton Trans. (1994) 735.
[31] Programs CRYSALIS-CCD and -RED, Oxford Diffraction Ltd., Abingdon, UK, 2005.
[32] (a) G.M. Sheldrick, SHELX97 – Programs for Crystal Structure Analysis: Structure Determination (SHELXS), University of Göttingen, Germany, 1997.;
(b) G.M. Sheldrick, SHELX97 – Programs for Crystal Structure Analysis: Refinement (SHELXL), University of Göttingen, Germany, 1997.
[33] E.P. Serjeant, B. Dempsey, Ionization Constants of Organic Acids in Aqueous Solution, Pergamon, Oxford, 1979.
[34] G. Bandoli, A. Dolmella, Coord. Chem. Rev. 209 (2000) 161.
[35] G.J. Palenik, Inorg. Chem. 9 (1970) 2424.
[36] Y.J. Wu, S.Q. Huo, Y.J. Zhu, Organomet. Chem. 485 (1995) 61.
[37] K. Kunz, G. Erker, G. Kehr, R. Fröhlich, Organometallics 20 (2001) 392.
[38] A. Haaland, J.E. Nilsson, Acta Chem. Scand. 22 (1968) 2653.
[39] G. Zhang, H. Zhang, M. Sun, Y. Liu, X. Pang, X. Yu, B. Liu, Z. Li, J. Comput. Chem. 28 (2007) 2260.
[40] The Diamond software (Crystal Impact GbR, Bonn, Germany) was used for the molecular graphics in the Fig. 6.
[41] A. Haaland, Acc. Chem. Res. 12 (1979) 415.
[42] V.V. Strelets, Coord. Chem. Rev. 114 (1992) 1.
[43] (a) M.E.N.P.R.A. Silva, A.J.L. Pombeiro, J.J.R. Frausto da Silva, R. Herrmann, N. Deus, R.E. Bozak, J. Organomet. Chem. 480 (1994) 81;
(b) P. Stepnicka, L. Trojan, J. Kubista, J. Ludvik, J. Organomet. Chem. 637–639 (2001) 291;
(c) S.M. Batterjee, M.I. Marzouk, M.E. Aazab, M.A. El-Hashash, Appl. Organomet. Chem. 17 (2003) 291;
(d) M.L. Abasq, M. Saidi, J.L. Burgot, A. Darchen, J. Organomet. Chem. 694 (2009) 36.
[44] C. Hansch, A. Leo, R.W. Taft, Chem. Rev. 91 (1991) 165.
[45] Y.S. Sohn, D.N. Hendrickson, H.B. Gray, J. Am. Chem. Soc. 93 (1971) 3603.
[46] N. Rösch, K.H. Johnson, Chem. Phys. Lett. 24 (1974) 179.
[47] Y. Yamaguchi, W. Ding, C.T. Sanderson, M.L. Borden, M.J. Morgan, C. Kutal, Coord. Chem. Rev. 251 (2007) 515.
[48] Š. Toma, A. Gáplovská, M. Hudeček, Z. Langfelderová, Monatsh. Chem. 116 (1985) 357.
[49] E.A. Kassab, M.I. Marzouk, M. El-Hashash, J. Serb. Chem. Soc. 67 (2002) 593.
[50] P.A. Dowben, D.C. Driscoll, R.S. Tate, N.M. Boag, Organometallics 7 (1988) 305.
[51] T.Y. Dong, S.H. Lee, J. Organomet. Chem. 487 (1995) 77.
[52] H. Ju, B. Ye, J. Gu, Sensors 4 (2004) 71.
[53] P. Köpf-Maier, H. Köpf, E.W. Neuse, J. Cancer Res. Clin. Oncol. 108 (1984) 336.